Journal of Marine Systems 111–112 (2013) 253–262

Contents lists available at SciVerse ScienceDirect

Journal of Marine Systems

journal homepage: www.elsevier.com/locate/jmarsys

# Nutrient inputs to a Lagoon through submarine groundwater discharge: The case of Laoye Lagoon, Hainan, China

Tao Ji [a], Jinzhou Du [a,*], Willard S. Moore [b], Guosen Zhang [a], Ni Su [a], Jing Zhang [a]

[a] State Key Laboratory of Estuarine and Coastal Research, East China Normal University, Shanghai 200062, China
[b] Department of Earth and Ocean Sciences, University of South Carolina, Columbia, SC 29208, USA

ARTICLE INFO

*Article history:*
Received 24 April 2012
Received in revised form 12 November 2012
Accepted 20 November 2012
Available online 29 November 2012

*Keywords:*
Radium isotopes
Laoye Lagoon
Submarine groundwater discharge
Flushing time
Water age
Water budget
Nutrients

ABSTRACT

Submarine groundwater discharge (SGD) with inputs of nutrients in certain regions may play a significant role in controlling water quality in the coastal regions. In this paper, we have determined four naturally occurring radium isotope ($^{223}$Ra, $^{224}$Ra, $^{226}$Ra and $^{228}$Ra) activities and nutrient concentrations in surface water, coastal groundwater and river water in the mixing zone of Laoye Lagoon to estimate the fluxes of SGD by several models. The activities of the four radium isotopes of ground water were considerably greater than those in surface water samples. Using a $^{224}$Ra/$^{228}$Ra activity ratio (AR) model, we estimated the average lagoon water age to be 3.2 days, which was comparable with the flushing time of 4.0 days. Based on the excess radium isotopes and the water age of the lagoon, the estimated fluxes of SGD (in $10^6$ m$^3$/d) ranged from 2.64 to 5.32 with an average of 4.11. Moreover, we used Si balance to evaluate the flux of SGD ($4.8\times10^6$ m$^3$/d) which was close to the result calculated by radium. The SGD-derived nutrient fluxes (in mol/d) were DIN = $1.7\times10^5$, $PO_4^{3-} = 5.2\times10^2$, and $SiO_3 = 5.3\times10^4$. Furthermore, we applied the biogeochemical budget approach using $SiO_3$ as a tracer to evaluate the impact of SGD. The differences between the results estimated by radium and $SiO_3$ may indicate different pathways for the input of nutrients.



## 1. Introduction

Historically, submarine groundwater discharge (SGD) has been ignored as a source of nutrients to the coast. However, during the past two decades SGD has become recognized as a source of nutrients by many scientists (Burnett et al., 2001; Johannes, 1980; Moore, 1999; Simmons, 1992). Groundwater may be enriched in nutrients and heavy metals by natural causes and by the residential and agricultural development of near-shore areas, which lead to increased inputs of N and P from fertilizer and wastewater (Burnett et al., 2003; Johannes, 1980). Due to high nutrient concentrations in SGD, even a small SGD flux can transport a large flux of nutrients and other materials (Burnett et al., 2006; Corbett et al., 1999; Simmons, 1992; Slomp and Van, 2004). These nutrients released to estuarine and coastal surface waters by SGD may be of considerable importance for the ecology of some regions (Valiela et al., 1990); whereas, in other regions the nutrients from SGD are suggested to be the primary reason for water eutrophication (Paerl, 1997; Valiela et al., 2002). For example in Masan Bay, Korea, the fluxes of Si and P from SGD were 2–3 fold higher than that from stream water (Lee et al., 2009). As almost half of the population in the world is now living in the coastal zone and the ecosystems of these areas are relatively vulnerable (Jickells, 1998), it is very important to focus research on SGD.

For example, in the industrial coastal area of Zhejiang Province, Eastern China, a large amount of industrial wastewater, irrigation water, and sewage infiltrates into groundwater, raising the possibility that the nutrients in the polluted water may be discharged into the sea through SGD (Zhang, 2010). These industrial processes are augmented by mariculture, which causes N and P enrichment in local seawater. Being the fundamental elements for the growth of algae, excessive amounts of these nutrients may lead to coastal eutrophication, and even to harmful algae blooms. Such red tidal out-brakes have occurred nearly every year since the 1980s; and, this trend is becoming more severe with time in this coastal area (Hwang et al., 2005).

Although SGD is considered as one of the significant vectors that input nutrients, heavy metals, and other materials to the estuary and coast regions (Burnett et al., 1990, 2001; Corbett et al., 1999; Johannes, 1980; Moore, 1996, 1999; Valiela et al., 1990), work to quantify the sources of these materials are not adequate.

The flux of SGD has been demonstrated by many chemical tracers including $^{222}$Rn (Burnett and Dulaiova, 2003; Cable et al., 1996), methane (Corbett et al., 1999), barium (Moore, 1997) as well as radium isotopes (Moore, 1996, 2003). Among these methods, estimating SGD by Ra isotopes is one of the most efficient (Moore, 1996). There are four naturally occurring radium isotopes, i.e., $^{223}$Ra ($T_{1/2}$ = 11.4 days), $^{224}$Ra ($T_{1/2}$ = 3.6 days), $^{226}$Ra ($T_{1/2}$ = 1600 years), and $^{228}$Ra ($T_{1/2}$ = 5.7 years). Because of the large variation in the rates of generation and decay, these four isotopes can be used to study the

* Corresponding author. Tel.: +86 21 62232761; fax: +86 21 62546441.
*E-mail address:* jzdu@sklec.ecnu.edu.cn (J. Du).

0924-7963/$ – see front matter © 2012 Elsevier B.V. All rights reserved.
http://dx.doi.org/10.1016/j.jmarsys.2012.11.007

biogeochemical process with different time scales. For instance, the half-life of $^{224}$Ra is the shortest, so it is the best tracer for studying the migration rate of the seawater as well as the water exchange rate between the sediment interstitial water and the overlying seawater with the time scale of 1–10 days. On the other hand, $^{228}$Ra is used as a tracer for continental shelf influence in the sea with the time scale of 1–30 years (Zhang, 2007).

In order to evaluate the water quality and SGD flux in the ecosystem, we have applied Ra isotopes as tracers to estimate the SGD flux and the associated nutrient flux to Laoye Lagoon, Hainan, China, where the sea has been reclaimed for the development of aquaculture since 1970s (Sun, 2011). Building of dykes that trap the tidewater for mariculture reduces the connection between the lagoon and the sea. Many manmade shrimp ponds have been built since the 1980s, resulting in a mass of shrimp pond wastes being discharged into the lagoon (Sun, 2011). Furthermore, with the increase of agricultural, fishing, and tourism activities, the environment and ecosystem in Laoye Lagoon have been modified severely. These changes are suspected to be the cause of very serious red tides, which occurred in 1993, 1996 and 1999 in this area, causing huge economic losses (Sun, 2011). Therefore, this research could provide helpful information for understanding the disturbance from human activities and figuring out the baseline for the management to protect the ecosystem in this area.

## 2. Materials and methods

### 2.1. Study site

Hainan Island, the second largest island in China, is located at the south of China. Laoye Lagoon is one of the biggest lagoons in the southeast of Hainan Island, with an area of about 26 km$^2$. This spoon-shaped lagoon (Fig. 1) was formed in a transgression process in the Quaternary, and developed from sandbars. Along the east of this lagoon, large sandbars divide Laoye Lagoon from the South China Sea. Within the lagoon is an inner bay in the east (shaded by slash in Fig. 1), which is hardly affected by the tide; this is where the fish ponds are concentrated. In the southeast of the lagoon, there is a tidal channel about 8 km long and 200 m wide connecting to the sea. Because of sediment accumulation, the tidal channel is becoming smaller and shallower (Wang et al., 2006). Beyond the lagoon, there are long stretches of hills; the floodplain to the north of the lagoon is characterized by highly permeable alluvial sediment deposits, which constitute an area of high groundwater recharge that mainly comes from local precipitation (Ding et al., 2007). River flow into the lagoon was minimal during sampling time (April–May 2010) because of a lack of rainfall. We only found three rivers that flowed into the lagoon directly with a very slow velocity (~0.4 m/s).

The climate in Hainan is tropical monsoon, so it is warm all year round, the annual average temperature is ~26 °C. The annual average precipitation of Hainan Province is about 1600 mm, concentrated mostly from August to October, while the evaporation is strongest from May to July. It seldom rained during the sampling in April and May 2010. Hainan Island is abundant in tropical ecosystems such as mangroves, coral reefs and sea grass beds (Mao et al., 2006).

### 2.2. Methods

#### 2.2.1. Water samples

Surface water samples were collected from Laoye Lagoon using a submerged pump at a depth of 0.5 m below the surface. Groundwater samples were pumped from the wells, which were dug by the native habitants, along the shore utilizing the water pump. We also got river water samples by the water pump from the rivers that flow into the lagoon. All the samples were collected during the cruise in April 2010.

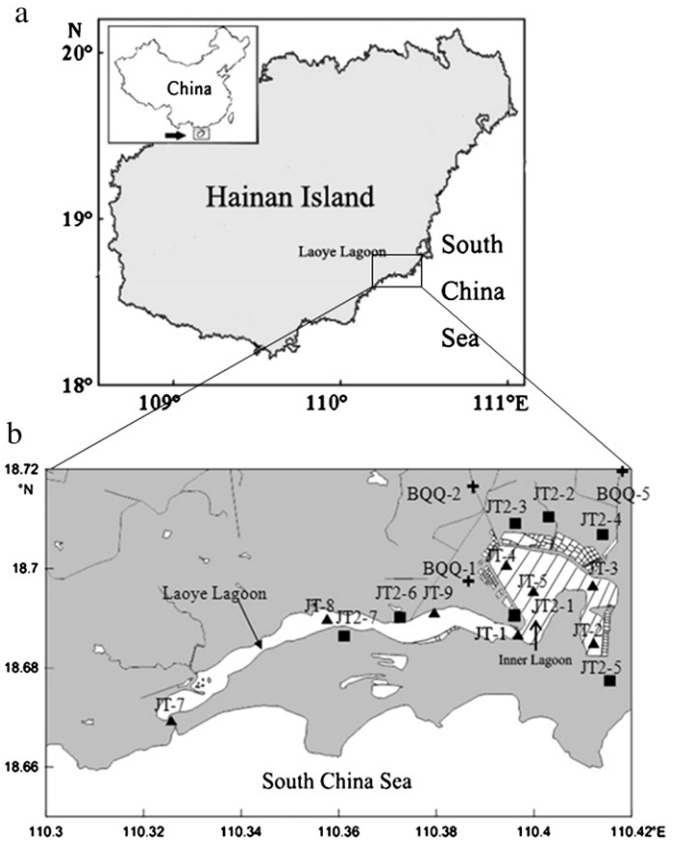


**Fig. 1.** Sampling location: (a) Hainan Island and (b) Laoye Lagoon; Sampling station: seawater (▲); groundwater (■) and river water (+). The inner bay is shaded by slash in the east of the lagoon. The stippled areas in the east of the lagoon are fish farms.

We collected 8 samples for surface water (60 L) and 7 samples for groundwater (20 L), as well as 3 samples for river water (60 L). We immediately filtered all the samples through cellulose acetate membranes with a pore size of 0.45 μm. Then the water samples were filtered through a column of Mn-fiber (20 g approximately) to absorb radium isotopes (Rama et al., 1987). The flow rates ranged from 1 to 2 L/min. We washed out the sea salt with DI water and controlled the moisture content of the fiber within 70%–80%. Then we immediately placed the column with Mn-fiber in the Radium Delayed Coincidence Counter (RaDeCC) to measure the short-lived isotope $^{224}$Ra (Moore and Amold, 1996). Each sample was again measured a week after collection to determine $^{223}$Ra. All the samples were analyzed for $^{228}$Th 5 weeks after collection on the same instrument to correct for supported $^{224}$Ra (Moore, 2008).

The long-lived $^{226}$Ra and $^{228}$Ra were measured about a year later by dissolving the Ra isotopes from the fiber with 200 ml hydroxylamine hydrochloride and 100 ml 1 M HCl plus a yield tracer of $^{225}$Ra in equilibrium with its parent, $^{229}$Th, (Eckert & Ziegler Isotope Products, 7229). The radium isotopes were separated following the radiochemical separation procedure of Hancock and Martin (1991). Briefly, a $Pb(NO_3)_2$ solution was added to the acidic solution described above and $Pb(Ra)SO_4$ was co-precipitated by adding 5 ml concentrated $H_2SO_4$ and 20 g solid $K_2SO_4$. The co-precipitate was centrifuged and redissolved in 0.1 M EDTA (PH = 10). After cooling, this solution was passed through an anion exchange column (DOWEX 1X8-200, 100–200 mesh, chloride form, 50 mm height, 7 mm i.d.) to remove Th and Ac. Then the eluate was passed through a cation exchange column (DOWEX 50WX8-200, 200–400 mesh, 80 mm height, 7 mm i.d.) to elute Pb, Ba and residual Th and Ac. Ra was eluted with 30 mL 6 M $HNO_3$. Finally, Ra was electrodeposited onto a stainless-steel disc at 120 mA for 30 min and determined by

α-particle spectrometry (Model: Canberra 7200–08). Because $^{226}$Ra is an α-emitting isotope, while $^{228}$Ra is a β-emitting isotope, the activity of $^{226}$Ra could be calculated immediately after the counting, but the activity of $^{228}$Ra could only be obtained after the disc was stored for more than 6 months to allow ingrowth of $^{228}$Th and $^{224}$Ra daughters and recounted.

#### 2.2.2. Nutrients

Water samples were collected with 2-L polyethylene bottles, then the samples were immediately filtered through 0.45 μm cellulose acetate filters that had been cleaned with hydrochloric acid (pH = 2) and rinsed with Milli-Q water. The filtrates were poisoned with saturated $HgCl_2$ and stored in the dark. The nutrient concentrations ($NO_2^-$, $NO_3^-$, $NH_4^+$, $PO_4^{3-}$ and $SiO_3$) were analyzed using an autoanalyzer (Model: Skalar SAN$^{plus}$) (Liu et al., 2005). The analytical precision was refer to the work carried out by Liu et al. (2009). The concentration of dissolved inorganic nitrogen (DIN) is the sum of $NO_2^-$, $NO_3^-$ and $NH_4^+$.

## 3. Results

### 3.1. Hydrological properties of Laoye Lagoon

The hydrological properties of sampling location are listed in Table 1. We can see that the depth of the lagoon is shallow, so the temperature of the surface water could be affected by sunlight. During the sampling time, the weather was sunny, the temperature of surface water changed comparatively large (range 27.3 °C to 29.6 °C) and the average water temperature was 27.9 °C, while the temperature of groundwater ranged from 27.3 °C to 28.1 °C, and the temperature of river water was a little higher, ranging from 29.5 °C to 33.9 °C.

A salinity gradient (ranging from 18 to 33‰) along the distance of the lagoon was observed during the sampling, with lower salinity inside of the lagoon and increasing salinity towards the mouth of the lagoon. Because of the narrow tidal channel, the salinity of the inner lagoon was similar (18–20.6‰), but it increased close to the mouth of the lagoon.

Fig. 2 shows the tidal periods and the tidal levels in Laoye Lagoon during the sampling time. We see that the tidal period was about 0.517 days, with the highest tidal level at 142 cm, and the lowest tidal level was 28 cm. The tidal level in this area is 90 cm below the mean sea level. The surface water in the tidal channel was certainly influenced by the tide.

### 3.2. The activities of Ra isotopes in surface water and groundwater

Since it was the pre-summer monsoon season in Hainan Island, there was little river water flowing into the lagoon. As a result, we could only find three rivers that flowed into the lagoon at a very slow velocity. The flow rate of the river was merely about 0.4 m/s and the flux of river was $5.2\times10^4$ m$^3$/d approximately. The salinity of the river water was constant for a long distance upstream, so it was very hard to find the river end-member. The river station BQQ-1 (salinity = 1.9‰) and BQQ-5 (salinity = 3.2‰) had very high radium levels, which may come from direct groundwater discharge into the river channel.

The salinity (‰) of the groundwater wells ranged from 0 to 0.3. Radium activities measured in the wells were mostly higher than that in the surface water. The highest radium isotope activities (in dpm/100 L) were $^{223}$Ra = 42, $^{224}$Ra = 760, $^{226}$Ra = 732, and $^{228}$Ra = 387. We got this sample (JT2-1) from the north of the lagoon where the aquifer is characterized by highly permeable alluvial sediment deposits.

The activities of Ra isotopes in surface water are shown in Table 1. In surface water of the lagoon, almost all the samples (salinity = 18–33‰) were significantly enriched in radium in comparison with those in seawater (Table 1). In our previous work (Su et al., 2011), we concluded that the high $^{226}$Ra activities of the lagoon water were due to the high-activity groundwater discharge. The radium activities near the lagoon mouth at the highest salinity (JT-7, salinity: 33‰) were the lowest, probably as a result of the dilution with the ocean and lower groundwater discharge. The radium activities of other sampling stations were much higher and salinity was lower, suggesting strong submarine groundwater discharge. Fig. 3a, b, c and d shows respectively the relationship between the activities of $^{223}$Ra, $^{224}$Ra, $^{226}$Ra, $^{228}$Ra and salinity for surface water of the lagoon. We see from these figures that the distributions of $^{223}$Ra and $^{224}$Ra are similar. The highest values were found in the tidal channel at a salinity of 23–28; the activities of $^{223}$Ra and $^{224}$Ra in the inner bay were lower with lower salinity. However, the distributions of $^{226}$Ra and $^{228}$Ra were different. Here, the highest values were found in the inner bay at a salinity of 18–21, and then decreased with increasing salinity closer to the mouth. This may reflect the shorter half-lives of $^{223}$Ra and $^{224}$Ra as the activities could change in the mixing zone as a result of regeneration and decay; conversely, the activities of long-lived $^{226}$Ra and $^{228}$Ra could only change by mixing with lower activity inner bay water after desorption is complete (Moore, 2003).

We see from Fig. 4a that $^{224}$Ra shows the same trend as $^{223}$Ra for groundwater except for station JT2-7, where $^{224}$Ra reached its highest

**Table 1**
Sampling stations and activities of radium isotopes (dpm/100 L) along with the longitude/latitude, salinity (‰), temperature (°C), and water depth (m) for all the water samples. The error for radium isotopes is one-sigma estimate.

| Station | Longitude (°N) | Latitude (°E) | Salinity | Temp. (°C) | depth (m) | ex$^{224}$Ra | Error | $^{223}$Ra | Error | $^{226}$Ra | Error | $^{228}$Ra | Error |
|---|---|---|---|---|---|---|---|---|---|---|---|---|---|
| JT-4 | 110.39 | 18.70 | 18.0 | 29.6 | 3.0 | 159 | 7.9 | 12.7 | 0.9 | 70.4 | 3.6 | 296 | 11.9 |
| JT-5 | 110.40 | 18.70 | 19.1 | 28.4 | 2.8 | 208 | 10.4 | 13.1 | 0.9 | 58.5 | 2.1 | 209 | 10.9 |
| JT-2 | 110.41 | 18.69 | 19.2 | 27.3 | 2.2 | 103 | 5.1 | 6.66 | 0.5 | 101 | 5.1 | 422 | 23.7 |
| JT-3 | 110.41 | 18.70 | 20.2 | 27.6 | 2.7 | 176 | 8.8 | 11.1 | 0.8 | 40.3 | 1.2 | 361 | 4.8 |
| JT-1 | 110.40 | 18.69 | 20.6 | 27.5 | 3.0 | 234 | 11.7 | 13.0 | 0.9 | 105 | 3.6 | 504 | 27.0 |
| JT-9 | 110.38 | 18.69 | 23.7 | 28.6 | 1.8 | 293 | 14.6 | 14.6 | 1.0 | 76.6 | 3.7 | 337 | 13.5 |
| JT-8 | 110.36 | 18.69 | 27.2 | 28.1 | 2.2 | 277 | 13.8 | 16.1 | 1.1 | 59.8 | 1.7 | 309 | 15.8 |
| JT-7 | 110.33 | 18.67 | 33.0 | 26.5 | 4.7 | 41.6 | 2.1 | 1.68 | 0.1 | 14.4 | 0.7 | 47.1 | 9.9 |
| JT2-7 | 110.36 | 18.69 | 0.0 | 27.3 | 4.5 | 546 | 27.3 | 11.58 | 0.8 | 224 | 4.8 | 422 | 14.3 |
| JT2-4 | 110.41 | 18.71 | 0.2 | 27.5 | 6.0 | 103 | 5.2 | 3.63 | 0.3 | 83.5 | 2.9 | 171 | 9.1 |
| JT2-5 | 110.42 | 18.68 | 0.2 | 27.3 | 8.0 | 23.8 | 1.2 | 1.78 | 0.1 | 13.1 | 0.5 | 33.8 | 2.0 |
| JT2-6 | 110.37 | 18.69 | 0.2 | 27.5 | 3.5 | 88.9 | 4.5 | 2.67 | 0.2 | 32.4 | 0.8 | 172 | 5.2 |
| JT2-1 | 110.40 | 18.69 | 0.3 | 28.1 | 3.0 | 759 | 37.9 | 42.1 | 3.0 | 277 | 13.1 | 865 | 40.1 |
| JT2-2 | 110.40 | 18.71 | 0.3 | 28 | 4.0 | 144 | 7.2 | 7.55 | 0.5 | 75.5 | 3.5 | 205 | 7.0 |
| JT2-3 | 110.40 | 18.71 | 0.3 | 27.4 | 10.0 | 312 | 15.5 | 18.53 | 1.3 | 264 | 6.4 | 409 | 20.3 |
| BQQ-2 | 110.39 | 18.72 | 0.0 | 33.2 | 0.3 | 3.52 | 0.2 | 0.52 | 0.0 | 2.01 | 0.2 | 2.79 | 0.2 |
| BQQ-1 | 110.39 | 18.70 | 1.9 | 29.5 | 0.3 | 183 | 9.2 | 3.06 | 0.2 | 201 | 5.5 | 189 | 7.3 |
| BQQ-5 | 110.42 | 18.72 | 3.2 | 33.9 | 0.2 | 440 | 22.0 | 14.7 | 1.0 | 407 | 26.2 | 314 | 12.1 |

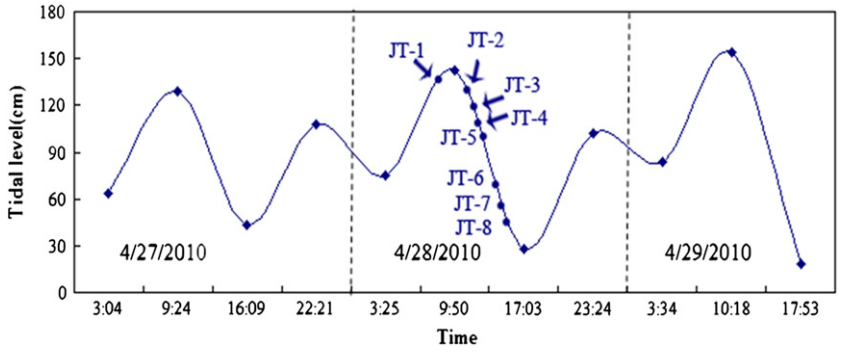


**Fig. 2.** Tidal level condition of Laoye Lagoon during the sampling time. Most of samples were collected in the ebb tide. The tidal level is 90 cm below mean sea level.

concentration. We learned that the local people exploited a large volume of groundwater for building houses. These activities might cause the high $^{224}$Ra level, as it regenerates more quickly than the other Ra isotopes.

### 3.3. The activity ratios of Ra isotopes in surface water and groundwater

Fig. 4a shows a strong linear relation of $^{224}$Ra vs. $^{223}$Ra for the surface water ($R^2 = 0.88$), groundwater ($R^2 = 0.79$, including JT2-7 which we discussed above) and river water ($R^2 = 0.94$). Fig. 4b is a plot of $^{228}$Ra vs. $^{226}$Ra for all samples. Although the geochemical behaviors of these two isotopes should be the same, the different half-lives affect the rates of their activity production from their parents, with $^{228}$Ra having a higher production rate. Moreover, compared with the similar desorption behaviors of $^{228}$Ra and $^{226}$Ra from suspended particles, the diffusion behaviors of $^{228}$Ra and $^{226}$Ra from bottom sediments are very different (Elsinger and Moore, 1984; Rengarajan et al., 2002). Thus, various sources of Ra produce different $^{228}$Ra/$^{226}$Ra AR. In the surface water, the slope of the fitting line was higher than that in the groundwater and river water.

Fig. 5 is a plot of $^{224}$Ra vs. $^{228}$Ra for all samples. The slopes for seawater, groundwater and river water are 0.55 ($R^2 = 0.21$), 0.9 ($R^2 = 0.92$) and 1.29 ($R^2 = 0.95$), respectively. This is probably due to $^{224}$Ra decay in surface samples, implying that the surface water samples vary in apparent age.

### 3.4. Nutrient concentration of surface water and groundwater

The nutrient concentrations (in μmol/L) in this system are listed in Table 2. The average concentrations of DIN, $PO_4^{3-}$ and $SiO_3$ for surface water are 15.6, 5.7, and 8.1, respectively. The average concentrations of DIN, $PO_4^{3-}$ and $SiO_3$ for groundwater are 218, 12, and 171, respectively. Compared to the surface water, the DIN and $SiO_3$ in groundwater were much higher, which may be related to mariculture and agricultural activities (Liu et al., 2007).

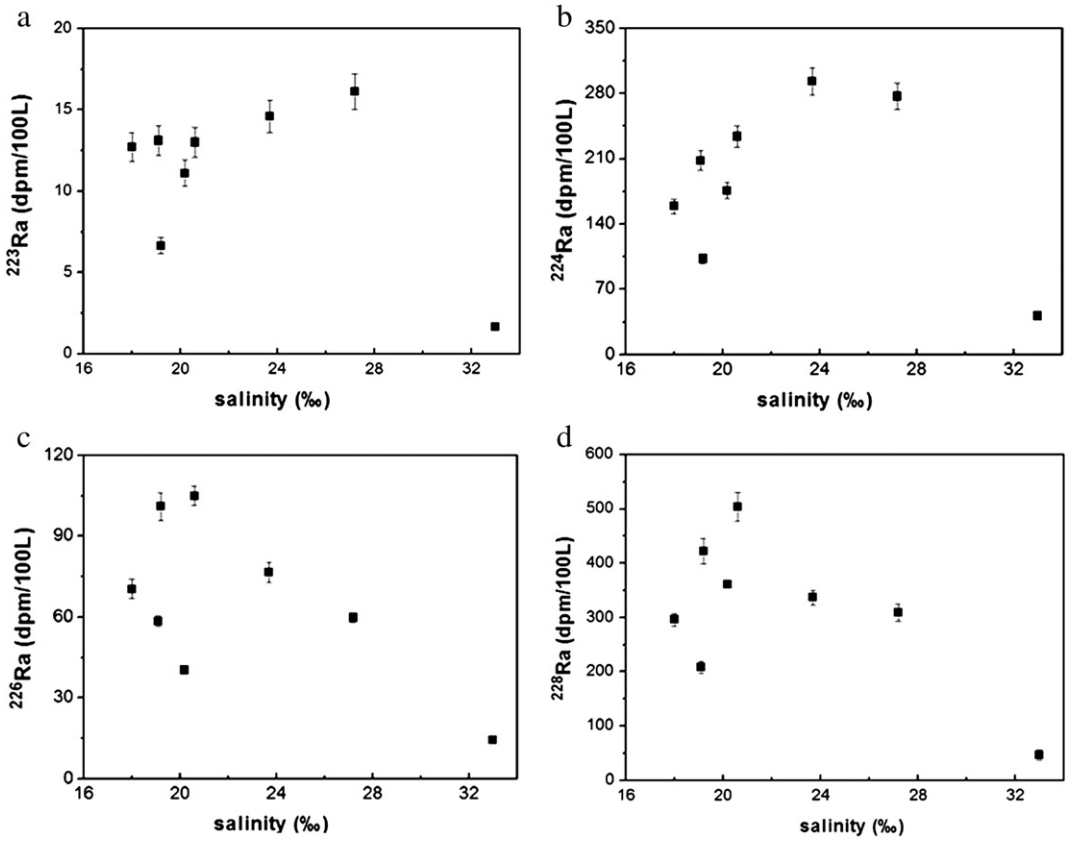


**Fig. 3.** Plots of activities of Ra isotopes vs. salinity: (a) $^{223}$Ra; (b) $^{224}$Ra; (c) $^{226}$Ra and (d) $^{228}$Ra for surface water of the lagoon.

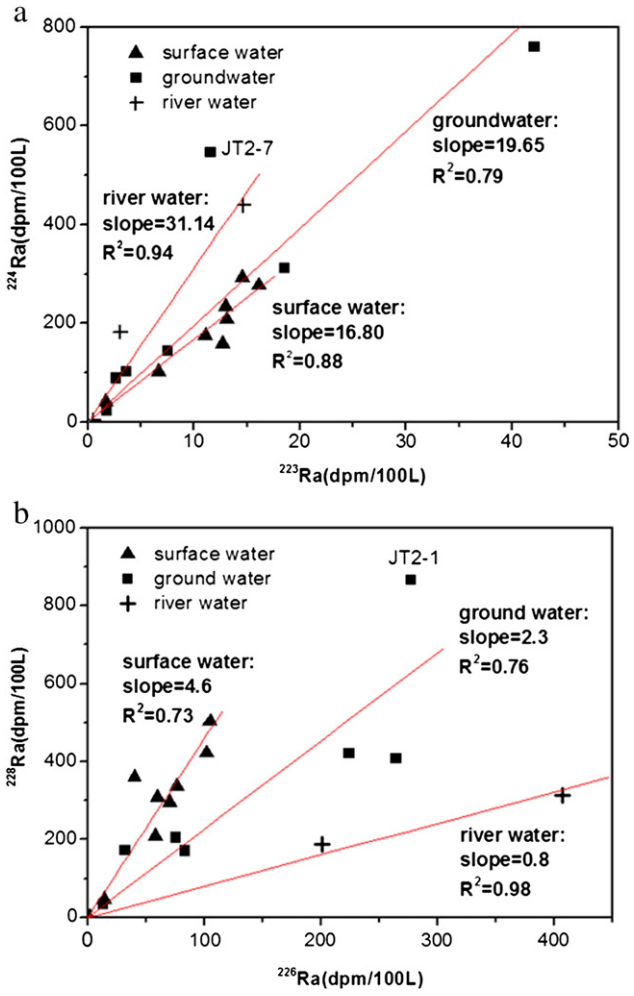


**Fig. 4.** Plot of (a) $^{224}$Ra vs $^{223}$Ra, (b) $^{228}$Ra vs $^{226}$Ra for all samples: surface water (▲); groundwater (■); and river water (+).

Fig. 6 shows plots of nutrient concentrations vs salinity. The relationship between the concentrations of DIN, $PO_4^{3-}$, $SiO_3$ and salinity was not obvious and did not exhibit conservative behavior. The maximum value of each nutrient appeared at a different salinity.

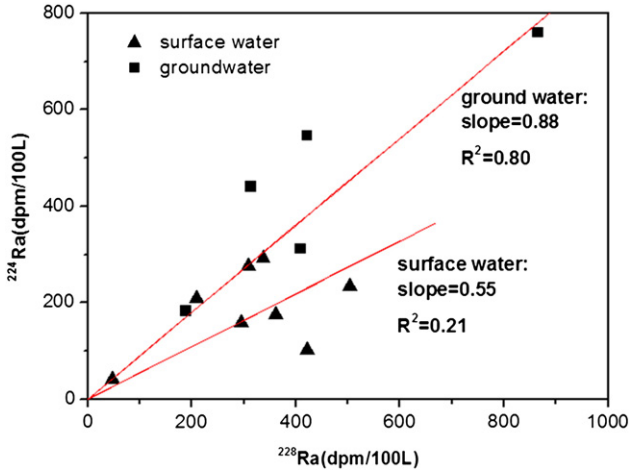


**Fig. 5.** Plot of $^{224}$Ra vs $^{228}$Ra for all the samples: surface water (▲); groundwater (■); and river water (+).

**Table 2**
The concentration of nutrients (μmol/L) and the radios of N/P as well as Si/N for all water samples; along with concentration of the dissolved oxygen (DO, μmol/L).

| Station | Salinity | $NO_2^-$ | $NH_4^+$ | $NO_3^-$ | DIN | $PO_4^{3-}$ | $SiO_3$ | N/P | Si/N | DO |
|---|---|---|---|---|---|---|---|---|---|---|
| JT-4 | 18.0 | 0.4 | 8.0 | 0.5 | 8.8 | 2.8 | 14.1 | 3.2 | 1.6 | 315 |
| JT-5 | 19.1 | 1.7 | 18.4 | 3.8 | 23.9 | 5.8 | 12.3 | 4.1 | 0.5 | 90.6 |
| JT-2 | 19.2 | 0.2 | 7.5 | 0.3 | 8.1 | 4.3 | 2.8 | 1.9 | 0.3 | 403 |
| JT-3 | 20.2 | 0.3 | 8.1 | 0.3 | 8.7 | 5.5 | 4.3 | 1.6 | 0.5 | 125 |
| JT-1 | 20.6 | 0.1 | 6.9 | 0.3 | 7.4 | 5.6 | 4.0 | 1.3 | 0.5 | 200 |
| JT-9 | 23.7 | 2.1 | 21.7 | 5.4 | 29.2 | 5.7 | 13.5 | 5.1 | 0.5 | 128 |
| JT-8 | 27.2 | 2.1 | 25.1 | 3.7 | 30.9 | 4.2 | 8.9 | 7.4 | 0.3 | 109 |
| JT-7 | 33.0 | 0.2 | 7.5 | 0.0 | 7.8 | 12 | 4.6 | 0.6 | 0.6 | 218 |
| JT2-7 | 0.0 | 0.1 | 2.5 | 73.0 | 75.6 | 0.1 | 39.6 | 526 | 0.5 | 215 |
| JT2-4 | 0.2 | 0.2 | 0.1 | 12.8 | 13.1 | 1.0 | 355 | 13.1 | 27.1 | 300 |
| JT2-5 | 0.2 | 1.0 | 1.6 | 149 | 151 | 13.3 | 177 | 11.4 | 1.2 | 168 |
| JT2-6 | 0.2 | 0.2 | 11.3 | 327 | 338 | 13.2 | 184 | 25.6 | 0.5 | 196 |
| JT2-1 | 0.3 | 0.2 | 20.1 | 45.5 | 65.8 | 0.2 | 20.4 | 345 | 0.3 | 37.5 |
| JT2-2 | 0.3 | 0.3 | 0.6 | 489 | 490 | 28.6 | 211 | 17.2 | 0.4 | 296 |
| JT2-3 | 0.3 | 3.2 | 1.3 | 389 | 393 | 28.4 | 207 | 13.8 | 0.5 | 290 |
| BQQ-2 | 0.0 | 0.8 | 1.7 | 3.9 | 6.4 | 1.8 | 1.2 | 36.2 | 1.8 | N/A |
| BQQ-1 | 1.9 | 0.7 | 5.0 | 0.7 | 6.4 | 2.0 | 53.6 | 31.4 | 0.8 | N/A |
| BQQ-5 | 3.2 | 0.2 | 3.5 | 0.3 | 4.0 | 0.1 | 20.9 | 52.3 | 5.2 | 121 |

## 4. Discussion

### 4.1. Three-end-member mixing model for radium balance

Moore (2003) developed a three-end-member mixing model based on the water, salinity and radium balances to estimate the fractions of seawater, groundwater and river water in an estuary. In this study we followed this model and constructed the equations for radium balance; we assumed that the diffusion of radium from the bottom sediment was negligible. We write equations for water, salt, and $^{226}$Ra balance.

$$f_S + f_{GW} + f_R = 1.00 \tag{1}$$

$$So = f_R \cdot S_R + f_S \cdot Ss + f_{GW} \cdot S_{GW} \tag{2}$$

$$^{226}Ra_O = {}^{226}Ra_S f_S + {}^{226}Ra_{GW} f_{GW} + {}^{226}Ra_R f_R \tag{3}$$

where $f$ is the fraction of the seawater ($S$), groundwater ($GW$) and river ($R$) end-members; $^{226}Ra_S$ is the $^{226}$Ra activity and $S_s$ is the salinity in the seawater end-member; $^{226}Ra_{GW}$ is the $^{226}$Ra activity and $S_{GW}$ is the salinity in the groundwater end-member; $^{226}Ra_R$ is $^{226}$Ra activity and $S_R$ is the salinity in the river end-member; and $^{226}Ra_O$ is the $^{226}$Ra activity and $S_O$ is the salinity measured in the sample.

According to Fig. 4b, the slope of the $^{228}$Ra vs. $^{226}$Ra of the groundwater samples is significantly lower than the slope of the surface water samples. Thus, input of the average groundwater cannot explain the $^{228}$Ra/$^{226}$Ra activity ratio (AR) in the surface water. However, one sample, JT2-1, does have approximately the necessary $^{228}$Ra/$^{226}$Ra AR to explain the surface water AR. Therefore, we use JT2-1 as the groundwater end-member (S = 0.3, $^{226}$Ra = 277 ± 13.1 dpm/100 L). We chose the water sample nearest the mouth (station JT-7) to represent the seawater end-member (S = 33, $^{226}$Ra = 14.4 ± 0.7 dpm/100 L) and the water sample from the station BQQ-2 to represent the river water end-member (S = 0.0, $^{226}$Ra = 2 ± 0.17 dpm/100 L). Eqs. (1) and (2) may be rewritten for the fractions of each end-member:

$$f_S = \frac{\left(\frac{^{226}Ra_O - {}^{226}Ra_R}{^{226}Ra_{GW} - {}^{226}Ra_R}\right) - \left(\frac{S_O - S_R}{S_{GW} - S_R}\right)}{\left(\frac{^{226}Ra_S - {}^{226}Ra_R}{^{226}Ra_{GW} - {}^{226}Ra_R}\right) - \left(\frac{S_S - S_R}{S_{GW} - S_R}\right)} \tag{4}$$

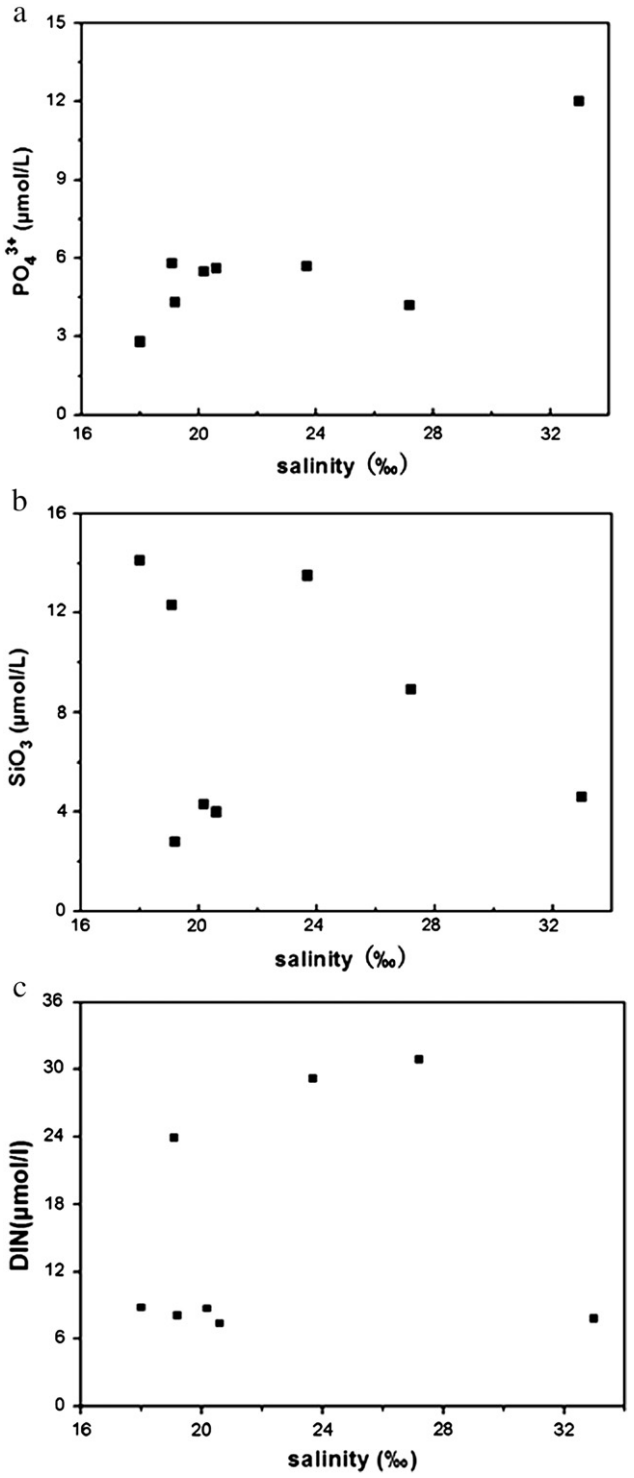


**Fig. 6.** Plots of nutrient concentration vs salinity for the surface water: (a) $PO_4^{3-}$; (b) $SiO_3$; and (c) DIN.

$$f_{GW} = \frac{S_O - S_R - f_S(S_S - S_R)}{S_{GW} - S_R} \quad (5)$$

$$f_R = 1 - f_S - f_{GW}. \quad (6)$$

Table 3 is the list of the fractions for each lagoon water samples; we can see that $f_S = 0.54$–$0.82$, $f_{GW} = 0.11$–$0.35$, $f_R = 0.01$–$0.28$. The average fractions were $f_S = 0.64$, $f_{GW} = 0.23$, and $f_R = 0.13$.

**Table 3**
Fractions of each end-member for the lagoon water samples.

| Station | $^{226}Ra$ | $f_S$ | $f_{GW}$ | $f_R$ |
|---|---|---|---|---|
| JT-1 | 105.11 | 0.62 | 0.35 | 0.03 |
| JT-2 | 101.86 | 0.58 | 0.34 | 0.08 |
| JT-3 | 40.25 | 0.61 | 0.11 | 0.28 |
| JT-4 | 70.35 | 0.54 | 0.23 | 0.23 |
| JT-5 | 58.52 | 0.58 | 0.18 | 0.24 |
| JT-8 | 59.81 | 0.82 | 0.17 | 0.01 |
| JT-9 | 76.55 | 0.72 | 0.24 | 0.04 |
| Average | 73.21 | 0.64 | 0.23 | 0.13 |

### 4.2. Ages and flushing times of surface water of Laoye Lagoon

Moore et al. (2006) developed a model to estimate the age of water in an estuary. In this model we assumed that radium additions and losses were constant and included radium fluxes from river and groundwater that were balanced by losses due to mixing and in the case of $^{224}Ra$, radioactive decay. We neglected fluxes from bottom sediments and suspended sediments. The equation for apparent water ages is

$$\tau_w = \left[F\left(^{224}Ra/^{228}Ra\right) - I\left(^{224}Ra/^{228}Ra\right)\right] / I\left(^{224}Ra/^{228}Ra\right)\lambda_{224} \quad (7)$$

Here $F(^{224}Ra/^{228}Ra)$ is the $^{224}Ra/^{228}Ra$ AR of the flux into the system, $I(^{224}Ra/^{228}Ra)$ is the $^{224}Ra/^{228}Ra$ AR in this system, $\lambda_{224}$ is the decay constant of $^{224}Ra$ (0.19 $d^{-1}$), and $\tau_w$ is the apparent age of water in this lagoon area. In this model, we chose the $^{224}Ra/^{228}Ra$ AR (0.88) from the JT2-1 groundwater sample as the initial $^{224}Ra/^{228}Ra$ AR because we assumed that the submarine groundwater discharge was the primary source of Ra isotopes to the lagoon system. Table 4 shows the age of each lagoon water sampling station which is based on the $^{224}Ra/^{228}Ra$ model.

The ages ranged from 0.02 to 13.76 days and the average apparent age was approximately 3.17 days. The range of ages was quite large. The distribution of ages indicates that the exchange process of the lagoon water is restricted toward the inner lagoon.

There is another way to estimate the "apparent age" of lagoon water. This is based on the flushing time, or the physical renewal capacity of the lagoon water (Baleo et al., 2001; Geyer et al., 2000) and produces a single value rather than a series of ages. We used the model developed by Sanford et al. (1992),

$$T_f = \frac{VT}{(1-b)P} \quad (8)$$

where $T_f$ is the flushing time, $V$ is the volume of the lagoon which is defined as the product of the average area and depth, $T$ is the tidal period, P is the tidal prism and $b$ is the return flow. We used the assumption of Moore et al. (2006), that the return flow can be estimated by the fraction of seawater in the lagoon ($f_S$), thus $f_S = b$.

**Table 4**
Water age based on the $^{224}Ra/^{228}Ra$ Model.

| Sample station | $^{224}Ra/^{228}Ra$ | Water age (days) | Sampling time | Tidal condition |
|---|---|---|---|---|
| JT-1 | 0.47 | 4.68 | 04/28/2010 9:20 | Flood tide |
| JT-2 | 0.24 | 13.76 | 04/28/2010 10:45 | Ebb tide |
| JT-3 | 0.49 | 4.24 | 04/28/2010 11:11 | Ebb tide |
| JT-4 | 0.54 | 3.38 | 04/28/2010 11:46 | Ebb tide |
| JT-5 | 1.00 | 0.62 | 04/28/2010 12:11 | Ebb tide |
| JT-7 | 0.88 | 0.02 | 04/28/2010 14:12 | Ebb tide |
| JT-8 | 0.9 | 0.09 | 04/28/2010 14:52 | Ebb tide |
| JT-9 | 0.87 | 0.07 | 04/28/2010 15:24 | Ebb tide |
| Average | 0.67 | 3.17 | | |

In order to estimate the tidal prism, we use data in Table 5, which gives the low tide and high tide mean water surface areas of $26\times10^6$ m$^2$ and $10\times10^6$ m$^2$, respectively. Thus the tidal prism is determined by integrating Eq. (9) from low tide to high tide, yielding $P=1.8\times10^7$ m$^3$. Since the width of the lagoon did not change significantly with the tide, the average volume of the lagoon could be assumed as a cuboid, to be approximately $5.0\times10^7$ m$^3$. With these parameters we estimate the average flushing time of the lagoon to be 3.99 days.

$$P=\int_H^0 Adz \tag{9}$$

where $A$ is the water surface area of the lagoon, and $z$ is the water depth over tidal range ($H$).

In summary, the average age and flushing time were 3.2 days and 4.0 days. After evaluating the uncertainties affected by the measurement errors, the accuracy of the model hypothesis and assumptions, we think the two estimates are comparable. We will use the flushing time to estimate the SGD flux to Laoye Lagoon.

### 4.3. SGD flux into the lagoon system

To quantify the SGD (submarine groundwater discharge) into the lagoon system, we follow the procedure of Moore et al. (2006) and construct a radium mass balance model in this lagoon system. The gains include the fluxes of groundwater and river water; the loss terms include mixing with other water bodies and the decay of short-lived isotopes ($^{223}$Ra and $^{224}$Ra). So we can write the following equations for $^{224}$Ra in this area:

$$F\left(^{224}Ra_{GW}\right)+F\left(^{224}Ra_R\right)=F\left(^{224}Ra_s\right)+F\left(^{224}Ra_{decay}\right). \tag{10}$$

Loss by decay:

$$F\left(^{224}Ra_{decay}\right)=V\left(^{224}Ra_O\right)\lambda_{224}. \tag{11}$$

Loss by mixing needs the data of the tidal prism. Considering the fraction of the water returned to the lagoon that did not mix with the sea, we can calculate the loss by mixing as:

$$F\left(^{224}Ra_s\right)=\frac{P}{T}\left[^{224}Ra_O-{}^{224}Ra_s-b\left(^{224}Ra_O-{}^{224}Ra_s\right)\right]. \tag{12}$$

**Table 5**
Summary of parameters for calculating the flushing time and water ages. Here $f$ is the fraction of the seawater ($S$), groundwater ($GW$) and river ($R$) end-members.

| Parameters | Values |
|---|---|
| Fractions of each end-member | |
| $f_S$ | 0.64 |
| $f_{GW}$ | 0.23 |
| $f_R$ | 0.13 |
| Average 224Ra/228Ra AR | |
| $^{224}$Ra/$^{228}$Ra AR (surface water) | 0.55 |
| $^{224}$Ra/$^{228}$Ra AR (groundwater) | 0.88 |
| $^{224}$Ra/$^{228}$Ra AR (river water) | 1.29 |
| High tide water surface area, $10^6$ m$^2$ | 26 |
| Low tide water surface area, $10^6$ m$^2$ | 10 |
| Mean water depth, m | 2.8 |
| Tidal period, days | 0.517 |
| Tidal range, m | 1.14 |
| $f_S=b$ | 0.64 |

Note that this equation is slightly different from the one used by Moore et al. (2006) because it does not employ a simplification used in the original equation. We combine Eqs. (10)–(12):

$$F\left(^{224}Ra_{GW}\right)+F\left(^{224}Ra_R\right)=\frac{P}{T}\left[^{224}Ra_O-{}^{224}Ra_s-b\left(^{224}Ra_O-{}^{224}Ra_s\right)\right]+V\left(^{224}Ra_s\right)\lambda_{224} \tag{13}$$

where $P$ is volume of the tidal prism, $T$ is tidal period, $b$ is the return flow, $V$ is the volume of the lagoon, $F(^{224}Ra_{GW})$ is the flux from groundwater, $F(^{224}Ra_R)$ is the flux from river water, $^{224}Ra_R$ is the $^{224}$Ra activity of the river, $^{224}Ra_{GW}$ is the $^{224}$Ra activity of the groundwater, $^{224}Ra_s$ is the $^{224}$Ra activity of the seawater, $^{224}Ra_{decay}$ is the decay of $^{224}$Ra, and $^{224}Ra_O$ is the $^{224}$Ra activity measured in the lagoon, here we use the mean $^{224}$Ra activity of the lagoon water (JT-1,2,3,4,5,8,9). The decay can be ignored for long-lived isotopes, so we can write similar equations for $^{226}$Ra and $^{228}$Ra.

$$F\left(^{226}Ra_{GW}\right)+F\left(^{226}Ra_R\right)=\frac{P}{T}\left[^{226}Ra_O-{}^{226}Ra_s-b\left(^{226}Ra_O-{}^{226}Ra_s\right)\right] \tag{14}$$

$$F\left(^{228}Ra_{GW}\right)+F\left(^{228}Ra_R\right)=\frac{P}{T}\left[^{228}Ra_O-{}^{228}Ra_s-b\left(^{228}Ra_O-{}^{228}Ra_s\right)\right] \tag{15}$$

$$SGD=\frac{FRa_{GW}}{Ra_{GW}} \tag{16}$$

The flux of the radium isotopes is obtained by dividing the radium inventory (I) by the flushing time ($T_f$). To calculate the inventory, we used the average radium activities and volume of the lagoon system and assumed that the water column was mixed vertically (Liu et al., 2011). The $^{224}$Ra, $^{226}$Ra and $^{228}$Ra activities (dpm/100 L) of groundwater (from sample JT2-1) are 759, 277, and 865; the average $^{224}$Ra, $^{226}$Ra and $^{228}$Ra activities of lagoon water are 207, 73.1, and 348; the $^{224}$Ra, $^{226}$Ra and $^{228}$Ra activities (dpm/100 L) of seawater (from sample JT-7) are 41.6, 14.4 and 47.1; and the average $^{224}$Ra, $^{226}$Ra and $^{228}$Ra activities of river water are 3.52, 2.01, and 2.79. The influence of the river is so small that we can ignore it. The fluxes ($10^{10}$ dpm/d) of $^{224}$Ra, $^{226}$Ra and $^{228}$Ra (from Eqs. (13)–(15)) are 4.04, 0.73, and 3.77. According to Eq. (16), these data yield the SGD rates ($10^6$ m$^3$/d) of 5.32, 2.64, and 4.36, with an average of $4.11\times10^6$ m$^3$/d. Compared with the flow of river water, SGD can be considered to be the major part of the terrestrially-derived water budget. We got the estimated flux of SGD by $^{226}$Ra-mass balance model to be $2.64\times10^6$ m$^3$/d, that is 0.1 m$^3$/m$^2\cdot$d if divided by the average area of lagoon ($18\times10^6$ m$^2$). Table 6 is a summary of SGD of lagoon worldwide. We could conclude that the flux of SGD in Laoye Lagoon is relatively high compared with other regions such as Venice Lagoon and Lesina Lagoon in Italy (Rapaglia et al., 2010, 2012).

We can also calculate the flux of SGD using the results of the 3 end-member mixing model:

$$SGD=\frac{Vf_{GW}}{T_f}. \tag{17}$$

Here $V=5.0\times10^7$ m$^3$, $f_{GW}=0.23$ (from Eq. (5)), and $T_f=4.0$ d, so we can estimate the flux of SGD to be $2.88\times10^6$ m$^3$/d, which is somewhat smaller than the average value we calculated above, but within the error, the same as the $^{226}$Ra-mass balance model.

We may also compare these Ra mass balance calculations with the results evaluated by other tracers such as Silicon (Kim et al., 2008). In order

**Table 6**
Summary of SGD of lagoon worldwide.

| Research area | Tracer | Activity (dpm/100 L) | SGD ($m^3/m^2 \cdot d$) | Reference |
|---|---|---|---|---|
| Coastal salt ponds, southern Rhode Island, US | $^{226}Ra$ | 16–77 | $0.1–0.3\times10^{-2}$ | Scott and Moran, 2001 |
| Patos–Mirim Lagoon, Brazil | $^{228}Ra$ | 15–21 | 3.5 | Niencheski et al., 2007 |
| Northern Venice lagoon, Italy | $^{226}Ra$ | 23–31 | $5\times10^{-2}$ | Garcia-Solsona et al., 2008 |
| Venice Lagoon, Italy | $^{226}Ra$ | 9.5–29.6 | $3–8\times10^{-2}$ | Rapaglia et al., 2010 |
| Southern Venice lagoon, Italy | $^{226}Ra$ | 34–69 | $0.4–1.1\times10^{-2}$ | Gattacceca et al., 2011 |
| Lesina Lagoon, Italy | $^{224}Ra$ | 30–193 | $0.8–5\times10^{-2}$ | Rapaglia et al., 2012 |
| Laoye Lagoon, China | $^{226}Ra$ | 40–101 | 0.1 | This study |

to estimate the SGD flux by Si, the chemical mass balance for Si can be expressed by the following equation (assuming Si mixes conservatively):

$$DSi_{EX} = DSi_O - f_{S1}DSi_S - (1-f_{S1})DSi_R. \quad (18)$$

In this system, we can rewrite Eq. (18) as:

$$f_{EX}DSi_{EX} = DSi_O - f_{S1}DSi_S - f_{R1}DSi_R \quad (19)$$

where $f_{S1}$, $f_{R1}$ and $f_{EX}$ are the fractions of the end-member of seawater, river water and excess Si, here $f_{S1}$ is calculated from the salinity of the measured values versus the salinity of seawater end-member. $DSi_{EX}$ is the excess concentration of Si; $DSi_S$ is the Si concentration in the seawater end-member; $DSi_R$ is Si concentration in the river end-member; and $DSi_O$ is the Si concentration measured in the sample. According to the analysis of radium in Section 4.1, we chose JT-7, JT2-1 and BQQ-2 as the seawater, groundwater and river water end-members respectively. The excess Si includes Si that could be taken into the lagoon system by groundwater, waste water and other sources. The concentrations (μmol/L) of Si in seawater, groundwater and river water end-members are 4.6, 20.4, and 1.15, respectively, thus the estimated $f_{S1}$, $f_{R1}$ and $f_{EX}$ are 0.64, 0.09 and 0.27. In a steady state, the amount of Si in Laoye Lagoon is a balance of fluxes of input and output of this system. The input terms include flux of river and excess Si, and the loss is mainly by mixing with the open sea:

$$F(DSi_{EX}) + \left[\frac{f_{R1}P}{T}(DSi_R)\right] = \left[\frac{f_{S1}P}{T}(DSi_s)\right] \quad (20)$$

$$SGD = \frac{FDSi_{EX}}{DSi_{EX}}. \quad (21)$$

Therefore, we estimate the SGD flux by Si balance to be $4.8\times10^6$ $m^3$/d which is somewhat higher than the $^{226}Ra$-mass balance model ($2.6\times10^6$ $m^3$/d), but in agreement with the $^{228}Ra$-mass balance model ($4.4\times10^6$ $m^3$/d). It is clear from each of the estimates that most of the radium and nutrients were contributed by groundwater, with rivers playing a minimal role.

### 4.4. Nutrient fluxes to Laoye Lagoon by SGD

Nutrient transport through the groundwater to the ocean has been shown to be a very significant component of the nutrient budget in coastal water (Costa et al., 2006; Garcia-Solsona et al., 2008). We have obtained the concentration of nutrients for surface water, groundwater and river water in this system (Table 2). No correlation was observed between concentrations of nutrients and radium activities. As Fig. 6 shows, there is no consistent relationship between the salinity and the concentrations of the DIN, $PO_4^{3-}$ and $SiO_3$.

The nutrient input through SGD into the lagoon can be evaluated by multiplying the SGD rates by the nutrient concentration of the SGD end-member. We again chose JT2-1 as the groundwater end-member, where the concentrations of DIN, $PO_4^{3-}$ and $SiO_3$ are 65.8 μmol/L, 0.2 μmol/L and 20.4 μmol/L respectively (Table 2). If we assume that this end-member represents the fluxes of nutrients into the lagoon, we can use our estimated SGD flux by $^{226}Ra$-mass balance model ($2.6\times10^6$ $m^3$/d) to estimate nutrient inputs. For DIN, $PO_4^{3-}$ and $SiO_3$, these are $1.7\times10^5$ mol/d, $5.2\times10^2$ mol/d, and $5.3\times10^4$ mol/d, respectively. We can compare these inputs with inventories in the lagoon to establish the minimum required inputs. Taking the average volume of the lagoon to be $5\times10^7$ $m^3$, the flushing time to be 4 days, and the DIN, $PO_4^{3-}$ and $SiO_3$ for lagoon water to be 16.7 μmol/L, 4.8 μmol/L and 8.6 μmol/L, respectively, we can estimate the fluxes required to support the measured inventories, assuming there is no biological removal. The required fluxes (in $10^4$ mol/day) for DIN, $PO_4^{3-}$ and $SiO_3$ are 4.3, 1.2, and 2.2, respectively. For DIN and $SiO_3$ the SGD fluxes are more than adequate to support the measured inventories; for $PO_4^{3-}$ the fluxes are not adequate. Either there are other sources of $PO_4^{3-}$ or there could have been an analytical problem with the analysis for JT2-1, as the $PO_4^{3-}$ concentration was unusually low.

Although this exercise demonstrated that the N and Si could be supplied by SGD, there may be considerable biological removal in the lagoon and there may be sources of nutrients that do not affect the radium fluxes significantly. We have simply shown that the assumptions, parameters, and models we have chosen can supply adequate N and Si. In addition to SGD the low quality of the water in this area may be influenced by the large number of shrimp ponds around the lagoon, which may discharge nutrient-rich water directly to the lagoon. These ponds also restrict water exchange, so the concentrations of $NO_2^-$, $NO_3^-$, $NH_4^+$, $PO_4^{3-}$ and $SiO_3$ become rather high. Furthermore, the narrow mouth is the only exchange channel with the open sea, causing enhanced degradation of the lagoon water.

Another method that can be used to evaluate the impact of SGD is the biogeochemical budget approach. A box model for this application was devised by Land Ocean Interactions in the Coastal Zone (LOICZ) to construct nutrient budgets from non-conservative distributions of nutrients and water budgets (Gordon et al., 1996; Liu et al., 2011). In this model, we assumed that the lagoon was in a steady state and it was treated as a single box which was well mixed both vertically and horizontally. Although this is not true, we approximate this condition by taking the means of the widely-distributed lagoon water samples. Eq. (22) expresses the water mass balance:

$$Q_{Re} = Q_{in} - Q_{out} = -dV/dt + Q_R + Q_P + Q_{GW} + Q_W - Q_E \quad (22)$$

where $Q_{Re}$ is denoted as the residual flow, which is equal to the net input of fresh water, $Q_{in}$ and $Q_{out}$ are the mean advective inflow and outflow of the water of the lagoon, V is the volume of the lagoon, $Q_R$, $Q_P$, $Q_{GW}$, $Q_W$, and $Q_E$ are the average flow rates of the river water, precipitation, groundwater, wastewater and evaporation. We assumed that the lagoon was in a steady state, and $V$ is $5\times10^7$ $m^3$, so $dV/dt = 0$. Table 7 gives us the data used in the calculation. In this lagoon system, the average $Q_E$ is $3.3\times10^4$ $m^3$/d (Li, 2010). We also assumed that the salinity values of the fresh water ($Q_R$, $Q_P$ and $Q_E$) were all zero. Since we did not know the flux of the waste water, the impact of the waste water can be unconsidered in this case. The salt balance in this system can be derived as follows:

$$Q_X(S_1 - S_2) = S_{Re}Q_{Re} + V * dS_1/dt + S_{GW}Q_{GW} \quad (23)$$

$$S_{Re} = (S_1 + S_2)/2 \quad (24)$$

**Table 7**
Summary of parameters for calculating SGD by $SiO_3$. Here $Q_E$ is the average flow rates of evaporation; $Q_X$ is mixing flow between the system of interest and the adjacent system; $S_1$ and $S_2$ are the average salinities in the system of interest and the adjacent system; $C_1$, $C_2$ and $C_{GW}$ are the average concentration of Si in the system of interest, adjacent ocean system and the groundwater discharge, respectively.

| Parameters | Values |
|---|---|
| $Q_E$, $\times 10^4$ $m^3$/d | 3.3 |
| $Q_X$, $\times 10^6$ $m^3$/d | 2.8 |
| $S_1$, ‰ | 21.1 |
| $S_2$, ‰ | 33.0 |
| $C_1$, μmol/L | 8.55 |
| $C_2$, μmol/L | 4.60 |
| $C_{GW}$, μmol/L | 114 |

where $S_1$ and $S_2$ are the average salinities in the system of interest and the adjacent system, $S_{GW}$ is the salinity of groundwater, $V$ is the volume of the system, and $Q_X$ is mixing flow between the system of interest and the adjacent system. The total water exchange time ($\tau$) of the system of interest can be estimated from the ratio $V/(Q_{Re}+Q_X)$; here we use the flushing time $T_f = 4.0$ days that we calculated above. The average salinity of interest system is 21.1. The adjacent system can be recognized as the ocean end-member, the salinity of which is 33.0 (Table 7). Thus $S_{Re}$ is 27.05.

Then $Q_{Re}$ is calculated to be $3.74\times10^6$ $m^3$/d and $Q_X$ is $8.76\times10^6$ $m^3$/d. So we can determine $Q_{GW} = 3.78\times10^6$ $m^3$/d, which is within error, the same as the result estimated by radium.

We now calculate the non-conservative fluxes of nutrient elements ($\Delta F$) based on water budgets and nutrient concentrations, here we take $SiO_3$ as an example:

$$\Delta F = \Sigma outflux - \Sigma influx = C_{Re}Q_{Re} + C_X Q_X - C_R Q_R - C_P Q_P - C_{GW}Q_{GW} \quad (25)$$

$$C_{Re} = (C_1 + C_2)/2 \quad (26)$$

$$C_X = C_1 - C_2 \quad (27)$$

where $C_{Re}$, $C_1$, $C_2$, $C_X$, $C_R$, $C_P$ and $C_{GW}$ are the average concentration of Si in the residual-flow boundary, system of interest, adjacent ocean system, mixing flow, the river runoff, precipitation and the groundwater discharge, respectively. From Table 7, we know that $C_1$ is 8.55 μmol/L, $C_2$ is 4.6 μmol/L, and $C_{GW}$ is 20.4 μmol/L. As a result, $C_{Re}$ is 6.58 μmol/L and $C_X$ is 3.95 μmol/L.

Because of the lack of rain and little inflow of river water, we can neglect $Q_R$ and $Q_P$. If we also neglect $Q_W$ (wastewater), we can regard the source of nutrients to the lagoon to be mainly from groundwater. As a result, the flux of $SiO_3$ is $1.8\times10^4$ mol/d, which is about a third of the Si flux we calculated above. This suggests that there may be other source of Si, such as wastewater. The wastewater and aquaculture effluents remain to be determined.

In this lagoon system, the N/P ratios in the lagoon water are significantly lower (3.4) than the Redfield ratio (16), but some of the ratios in the groundwater are significantly higher (25–500). If the P concentration in JT2-1 is correct, this sample has a N/P = 330. What produces the low N/P in the surface water in spite of a very high input ratio is unknown. The contribution of P from aquaculture waters (shrimp ponds) may be one of the sources (Liu et al., 2011). This question demands further research.

## 5. Conclusion

A 3-end-member mixing model based on the water, salinity and radium balances was used to estimate the fractions of seawater, groundwater and river water in Laoye Lagoon. Based on the fraction of the tidal prism that returns to the estuary on the next high tide, the flushing time was estimated for this lagoon. The return flow factor (b = 0.64) yields a flushing time of 4.0 days. Another model based on the changes of $^{224}Ra/^{228}Ra$ AR is used to determine the average water age of 3.2 days. A radium mass balance is used to estimate an average SGD flux of $4.11\times10^6$ $m^3$/d.

We also analyzed the nutrient (DIN, $PO_4^{3-}$ and $SiO_3$) concentrations of the samples in this area, and found high levels, especially for the groundwater. We used a box model devised by Land Ocean Interactions in the Coastal Zone (LOICZ) to construct nutrient budgets from non-conservative distributions of nutrients and water budgets. The $SiO_3$ balance was used to calculate a flux of SGD of $3.78\times10^6$ $m^3$/d, which is essentially the same as calculated by Ra. The flux of $SiO_3$ calculated by this approach is estimated as $1.8\times10^4$ mol/d, which is smaller than the result calculated by radium isotopes.

We conclude that SGD is the major source of the high levels of radium and nutrients in lagoon water. The cause of the extremely low N/P radios in the surface water is unknown, which needs further investigation.

## Acknowledgments

We would like to thank the lab colleagues for their field help. This research was supported by the Natural Science foundation of China (40830850), the State Key Laboratory of Estuarine and Coastal Research of China (SKLEC-2012KYYW05; 2010RCDW04) and the 111 project (B08022).

## References

Baleo, J.N., Humeau, P., Cloirec, P.L., 2001. Numerical and experimental hydrodynamic studies of a lagoon pilot. Water Res. 35 (9), 2268–2276.
Burnett, W.C., Dulaiova, H., 2003. Estimating the dynamics of groundwater input into the coastal zone via continuous radon-222 measurements. J. Environ. Radioact. 69 (1–2), 21–35.
Burnett, W.C., Cowart, J.B., Deetae, S., 1990. Radium in the Suwannee River and estuary-spring and river input to the Gulf of Mexico. Biogeochemistry 10, 237–255.
Burnett, W.C., Kim, G., Lane-Smith, D., 2001. A continuous radon monitor for assessment of radon in coastal ocean waters. J. Radioanal. Nucl. Chem. 249, 167–172.
Burnett, W.C., Bokuniewicz, H., Huettel, M., Moore, W.S., 2003. Groundwater and pore water inputs to the coastal zone. Biogeochemistry 66, 3–33.
Burnett, W.C., Aggarwal, P.K., Aureli, A., Bokuniewicz, H., Cable, J.E., 2006. Quantifying submarine groundwater discharge in the coastal zone via multiple methods. Sci. Total. Environ. 367, 498–543.
Cable, J.E., Burnett, W.C., Chanton, J.P., Weatherly, G., 1996. Estimating groundwater discharge into the northeastern Gulf of Mexico using radon-222. Earth Planet. Sci. Lett. 144, 591–604.
Corbett, D.R., Chanton, J.P., Burnett, W.C., Dillon, K., Rutkowski, C., Fourqurean, J.W., 1999. Patterns of groundwater discharge into Florida Bay. Limnol. Oceanogr. 44 (4), 1045–1055.
Costa Jr., O.S., Attrill, M.J., Nimmo, M., 2006. Seasonal and spatial controls on the delivery of excess nutrients to nearshore and offshore coral reefs of Brazil. J. Mar. Syst. 60 (1–2), 63–74.
Ding, S.J., Liao, X.J., Feng, Y.S., Xu, Z.S., 2007. Geological Environment in Northeastern Hainan Island. Geology Press, Beijing, p. 66 (in Chinese).
Elsinger, R.J., Moore, W.S., 1984. $^{226}Ra$ and $^{228}Ra$ in the mixing zones of the Pee Dee River-Winyah Bay, Yangtze River and Delaware Bay Estuaries. Estuarine Coastal Shelf Sci. 18 (6), 601–613.
Garcia-Solsona, E., Masqué, P., Garcia-Orellana, J., Rapaglia, J., Beck, A.J., Cochran, J.K., Bokuniewicz, H.J., Zaggia, L., Collavini, F., 2008. Estimating submarine groundwater discharge around Isola La Cura, northern Venice Lagoon (Italy), by using the radium quartet. Mar. Chem. 109, 292–306.
Gattacceca, J.C., Mayer, A., Cucco, A., Claude, C., Radakovitch, O., Vallet-Coulomb, C., Hamelin, B., 2011. Submarine groundwater discharge in a subsiding coastal lowland: a $^{226}Ra$ and $^{222}Rn$ investigation in the Southern Venice lagoon. Appl. Geochem. 26 (5), 907–920.
Geyer, W.R., Morris, J.T., Pahl, F.G., Jay, D.A., 2000. Interaction between physical processes and ecosystem structure: a comparative approach. Estuary Science: a Synthetic Approach to Research and Practice. Island Press, Washington D.C., pp. 177–206.

Gordon Jr., D.C., Boudreau, P.R., Mann, K.H., Ong, J.E., Silvert, W.L., Smith, S.V., Wattayakorn, G., Wuin, F., Yanagi, T. (Eds.), 1996. LOIZE Biogeochemical Modelling Guidelines: LOIZE Reports and Studies, 5. LOIZE, Texel, The Netherlands, p. 96.
Hancock, G.J., Martin, P., 1991. Determination of Ra in environmental samples by alpha-particle spectrometry. Appl. Radiat. Isot. 42, 63–69.
Hwang, D.W., Kim, G., Lee, Y.W., Yang, H.S., 2005. Estimating submarine inputs of groundwater and nutrients to a coastal bay using radium isotopes. Mar. Chem. 96, 61–71.
Jickells, T.D., 1998. Nutrient biogeochemistry of the coastal zone. Science 281 (5374), 217–222.
Johannes, R.E., 1980. The ecological significance of the submarine discharge of groundwater. Mar. Ecol. Prog. Ser. 3, 365–373.
Kim, G., Ryu, J.W., Hwang, D.W., 2008. Radium tracing of submarine groundwater discharge (SGD) and associated nutrient fluxes in a highly-permeable bed coastal zone, Korea. Mar. Chem. 109 (3–4), 307–317.
Lee, Y.W., Hwang, D.W., Kim, G., Lee, W.C., Oh, H.T., 2009. Nutrient inputs from submarine groundwater discharge (SGD) in Masan Bay, an embayment surrounded by heavily industrialized cities, Korea. Sci. Total. Environ. 407, 3181–3188.
Li, R.H., 2010. Nutrient Dynamics along Coastal Ecosystems of East Hainan [D]. Ocean University of China [D], Qingdao, p. 133 (in Chinese).
Liu, S.M., Zhang, J., Chen, H.T., Zhang, G.S., 2005. Factors influencing nutrient dynamics in the eutrophic Jiaozhou Bay, North China. Prog. Oceanogr. 66, 66–85.
Liu, G.Q., Wang, S.Y., Zhu, X.J., Liu, S.M., Zhang, J., 2007. Groundwater and nutrient discharge into Jiaozhou Bay, North China. Water Air Soil Pollut. Focus 7, 593–605.
Liu, S.M., Hong, G.H., Zhang, J., Ye, X.W., Jiang, X.L., 2009. Nutrient budgets for large Chinese estuaries. Biogeosciences 6, 2245–2263.
Liu, S.M., Li, R.H., Zhang, G.L., Wang, D.R., Du, J.Z., Herbeck, L.S., 2011. The impact of anthropogenic activities on nutrient dynamics in the tropical Wenchanghe and Wenjiaohe Estuary and Lagoon system in East Hainan, China. Mar. Chem. 125, 49–68.
Mao, L.M., Zhang, Y.L., Bi, H., 2006. Modern pollen deposits in coastal mangrove swamps from northern Hainan Island, China. J. Coast. Res. 22 (6), 1423–1436.
Moore, W.S., 1996. Large groundwater inputs to coastal waters revealed by $^{226}$Ra enrichments. Nature 380, 612–614.
Moore, W.S., 1997. The effects of groundwater input at the mouth of the Ganges–Brahmaputra Rivers on barium and radium fluxes to the Bay of Bengal. Earth Planet. Sci. Lett. 150, 141–150.
Moore, W.S., 1999. The subterranean estuary: a reaction zone of groundwater and seawater. Mar. Chem. 65, 111–125.
Moore, W.S., 2003. Sources and fluxes of submarine groundwater discharge delineated by radium isotopes. Biogeochemistry 66, 75–93.
Moore, W.S., 2008. Fifteen years experience in measuring $^{224}$Ra and $^{223}$Ra by delayed-coincidence counting. Mar. Chem. 109, 188–197.
Moore, W.S., Amold, R., 1996. Measurement of $^{223}$Ra and $^{224}$Ra in coastal waters using a delayed coincidence counter. J. Geophys. Res. 101, 1321–1329.
Moore, W.S., Blanton, J.O., Joye, S.B., 2006. Estimates of flushing times, submarine groundwater discharge, and nutrient fluxes to Okatee River, South Carolina. J. Geophys. Res. 111 (C9), C09006 http://dx.doi.org/10.1029/2005JC003041.
Niencheski, L.F.H., Windom, H.L., Moore, W.S., Jahnke, R.A., 2007. Submarine groundwater discharge of nutrients to the ocean along a coastal lagoon barrier, Southern Brazil. Mar. Chem. 106, 546–561.
Paerl, H.W., 1997. Coastal eutrophication and harmful algal blooms: importance of atmospheric deposition and groundwater as “new” nitrogen and other nutrient sources. Limnol. Oceanogr. 42, 1154–1165.
Rama, Todd, J.F., Butts, J.L., Moore, W.S., 1987. A new method for the rapid measurement of $^{224}$Ra in natural waters. Mar. Chem. 22, 43–54.
Rapaglia, J., Ferrarin, C., Zaggia, L., Moore, W.S., Umgiesser, G., Garcia-Solsona, E., Garcia-Orellana, J., Masqué, P., 2010. Investigation of residence time and groundwater flux in Venice Lagoon: comparing radium isotope and hydrodynamical models. J. Environ. Radioact. 101, 571–581.
Rapaglia, J., Koukoulas, S., Zaggia, L., Lichter, M., Manfé, G., Vafeidis, A.T., 2012. Quantification of submarine groundwater discharge and optimal radium sampling distribution in the Lesina Lagoon, Italy. J. Mar. Syst. 91, 11–19.
Rengarajan, R., Sarin, M.M., Somayajulu, B.L.K., Suhasini, R., 2002. Mixing in the surface waters of the western Bay of Bengal using $^{228}$Ra and $^{226}$Ra. J. Mar. Res. 60, 255–279.
Sanford, L.P., Boicourt, W.C., River, S.R., 1992. Model for estimating tidal flushing of small embayments. J. Waterw. Port Coastal Ocean Eng. 118, 635–654.
Scott, M.K., Moran, S.B., 2001. Ground water input to coastal salt ponds of southern Rhode Island estimated using $^{226}$Ra as a tracer. J. Environ. Radioact. 54 (1), 163–174.
Simmons Jr., G.M., 1992. Importance of submarine groundwater discharge (SGWD) and seawater cycling to material flux across sediment/water interfaces in marine environments. Mar. Ecol. Prog. Ser. 84, 173–184.
Slomp, C.P., Van, C.P., 2004. Nutrient inputs to the coastal ocean through submarine groundwater discharge: controls and potential impact. J. Hydrol. 295, 64–86.
Su, N., Du, J.Z., Moore, W.S., Liu, S.M., Zhang, J., 2011. An examination of groundwater discharge and the associated nutrient fluxes into the estuaries of eastern Hainan Island, China using $^{226}$Ra. Sci. Total. Environ. 409, 3909–3918.
Sun, Y.J., 2011. Application of Sedimentary Organic Biomarkers as Sources Tracer and Environmental Change Indicator: Case Studies in Hainan and the Rivers in the East of China [D]. East China Normal University, Shanghai, p. 45 (in Chinese).
Valiela, I., Costa, J., Foreman, K., Teal, J.M., Howes, B., Aubrey, D., 1990. Transport of groundwater-borne nutrients from watersheds and their effects on coastal waters. Biogeochemistry 10, 177–197.
Valiela, I., Bowen, J.L., Kroeger, K.D., 2002. Assessment of models for estimation of land-derived nitrogen loads to shallow estuaries. Appl. Geochem. 17, 935–953.
Wang, B.C., Chen, S.L., Gong, W.P., Ling, W.Q., Xu, Y., 2006. Development and Evolution of Estuarine Coast in Hainan Island. Ocean Press, Beijing . (in Chinese).
Zhang, L., 2007. Radium Isotopes in Changjiang Estuary and East China Sea and their Application in Analysis of Mixing among Multiple Water Masses [D]. East China Normal University, Shanghai, p. 7 (in Chinese).
Zhang, F., 2010. Influence of Submarine Groundwater Discharge on Nutrients Balance in Coastal Waters [D]. Zhejiang University, Hangzhou, p. 24 (in Chinese).